

# Migratory Aptitudes of Simple Alkyl Groups in the Anionotropic Rearrangement of Quaternary Chloromethyl Borate Species: A Combined Experimental and Theoretical Investigation

Andrea Bottoni,\* Marco Lombardo, Andrea Neri, and Claudio Trombini\*

Dipartimento di Chimica "G. Ciamician", Università di Bologna, via Selmi 2, 40126 Bologna, Italy

andrea@ciam.unibo.it; trombini@ciam.unibo.it

Received November 19, 2002

A combined experimental and theoretical investigation at the DFT and MP2 levels on the boron-to-carbon 1,2-shift in "ate species", coming from the quaternization of boranes (**A**) and boronate (**B**), is reported. To discuss the different migratory aptitudes of various alkyl groups, we have examined the migration of primary ( $R = \text{Me}$ ,  $\text{Et}$ ), secondary ( $R = i\text{-Pr}$ ), and tertiary ( $R = t\text{-Bu}$ ) alkyl groups. The effect of the counterion  $\text{Li}^+$  and of the solvent (polarized continuous model (PCM) method) has been considered. The following results are relevant: (a) in all cases, the reaction proceeds via a concerted-type mechanism which explains the retention of configuration at the migrating group and the inversion at the migration terminus experimentally observed. (b) The trend of the migration barriers along the direction primary  $\rightarrow$  secondary  $\rightarrow$  tertiary alkyl group observed in "ate" species **A** is reversed in boronate species **B**, in agreement with the experimental evidences. (c) A simple theoretical model is proposed where the barrier trend is the result of a delicate interplay between two opposite factors: (1) a "steric effect", which favors the most sterically demanding migrating groups, and (2) a "charge effect" associated with the partial carbanionic nature of the migrating carbon atom and which favors the less substituted migrating carbons.

## Introduction

The anionotropic rearrangement of a tetrasubstituted borate ion, via boron-to-carbon 1,2-shift, is at the basis of the most useful applications of organoboranes in organic synthesis. It is involved in the oxidation of boranes to give alcohols or amines as well as in a series of carbon-carbon bond-forming processes based on transient labile "ate" complexes.<sup>1-3</sup> The most outstanding feature of this process is the retention of configuration at the migrating group and the inversion at the migration terminus.<sup>4</sup> Both these evidences support a concerted-type mechanism. Despite the thousands of papers dealing with anionotropic rearrangements, a rationale of the factors governing the migratory aptitude of a boron substituent in an "ate" complex is still lacking. The only information we can find in the literature concerns the migratory aptitude scales of primary, secondary, and tertiary alkyl groups in well-defined reactions. Table 1 collects a few selected examples where two or three potential migrating groups are present in a transient "ate" species and the qualitative orders of migratory aptitude are reported. It is apparent that opposite migratory abilities are displayed by alkyl groups, mainly depending on the migration terminus (see entries 1 and 4). In many papers by the Brown group, the hexyl group<sup>5</sup> is used as a non-

migrating blocking group, for instance, in the carbonylation and cyanidation of trialkylboranes to give ketones<sup>6</sup> or in the haloalkyne route to disubstituted *E*-alkenes, trisubstituted alkenes, and ketones.<sup>7</sup> It is interesting to point out that methyl and hexyl groups, opposite substituents in terms of steric demand, often share the property of a nonmigrating group.

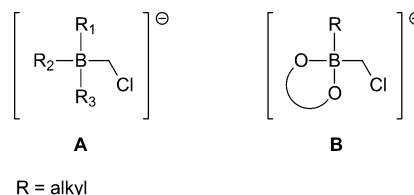


**FIGURE 1.** Schematic representation of the quaternary species deriving from boranes (**A**) and boronates (**B**).

Since the mechanistic scenario is rather confused, a model able to predict a migratory aptitude scale of simple alkyl groups is still lacking, and to our knowledge, no accurate computations on this reaction are available in the literature, we have carried out a combined experimental and theoretical investigation at the DFT and MP2 levels of the boron-to-carbon 1,2-shift in quaternary species deriving from boranes (**A**) and boronates (**B**), respectively (Figure 1).

(1) Cragg, G. M. L.; Koch, K. R. *Chem. Soc. Rev.* **1977**, 6, 393.

(2) Weill-Raynal, J. *Synthesis*, **1976**, 633.

(3) (a) Matteson, D. S. *CHEMTECH* **1999**, 6. (b) Matteson, D. S. *Chem. Rev.* **1989**, 89, 1535; (c) Matteson, D. S. *Tetrahedron* **1989**, 45, 1859.

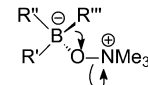
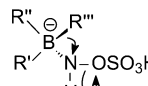
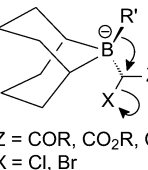
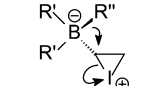
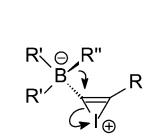
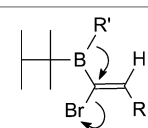
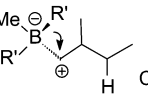
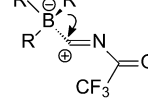
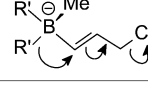
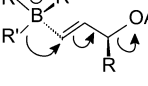
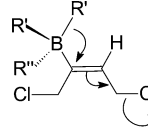
(4) Midland, M. M.; Zolopa, A. R.; Halterman, R. L. *J. Am. Chem. Soc.* **1979**, 101, 248.

(5) Negishi, E.; Brown, H. C. *Synthesis* **1974**, 77.

(6) Brown, H. C.; Bakshi, R. K.; Singaram, B. *J. Am. Chem. Soc.* **1988**, 110, 1529.

(7) Brown, H. C.; Basavaiah, D. *J. Org. Chem.* **1982**, 47, 754.

**TABLE 1. Selected Examples of Migratory Aptitude Orders of Alkyl Groups in Transient “Ate” Boron Species**

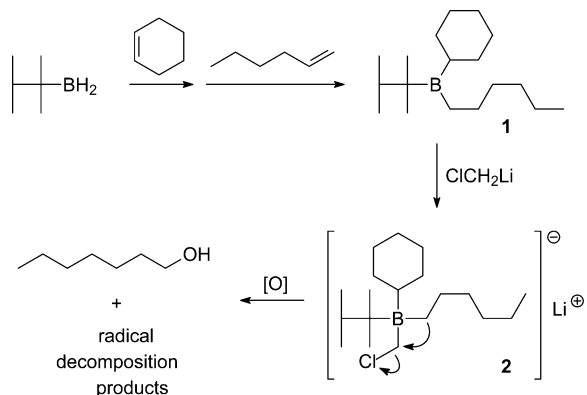
Entry	Transient “ate” species	Migratory Aptitude Scale	Ref
1		3° > 2° > 1°	8
2		2° > 1° isopinocampheyl > cyclohexyl methyl = non-migrating group	9
3	 Z = COR, CO <sub>2</sub> R, CN X = Cl, Br	R' = 1°, 2°, cycloalkyl R' = <i>i</i> -propyl, <i>t</i> -butyl 9-BBN = non-migrating group	10 11
4		2° > 1° > 3° cyclohexyl > <i>s</i> -butyl > <i>i</i> -butyl > <i>n</i> -butyl > bicyclooctyl > hexyl	12
5		1° > 2° > 3° bicyclooctyl > <i>n</i> -butyl > cyclohexyl = <i>s</i> -butyl ≈ <i>i</i> -butyl > hexyl <i>s</i> -butyl ≈ siamyl > cyclopentyl > isopinocampheyl	13 14
6		R' = 2-substituted 1°, 2°, cycloalkyl hexyl = non-migrating group	15
7		R' = 2° or cycloalkyl methyl = non-migrating group	16
8		1° > 2° > 3° hexyl = non-migrating group	17
9		R' = 2° or cycloalkyl methyl = non-migrating group	18
10		cyclohexyl > hexyl	19
11		R' = siamyl, cycloalkyl R'' = methyl or butyl, both non-migrating groups	20

## Results and Discussion

**A. Experimental Studies on Boranes.** A first triplicate experiment (Scheme 1) was designed, aimed at checking on a qualitative basis the migratory aptitude scale of alkyl groups in quaternary “ate” species **A**, deriving from boranes.

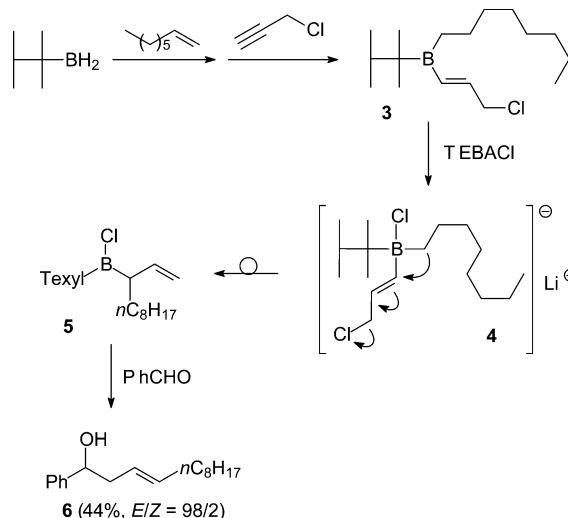
To this purpose, the Matteson homologation protocol of boronates<sup>3</sup> was applied to a simple mixed trialkyl-

borane. Hexylborane<sup>21</sup> was used in a two-step hydroboration sequence with cyclohexene and 1-hexene to give hexylcyclohexylhexylborane (**1**).<sup>22</sup> Quaternization of **1** to **2** was carried out according to the Matteson protocol<sup>23</sup> by adding *n*-butyllithium at −78 °C to a THF solution of ClCH<sub>2</sub>I and **1**. The bath was allowed to warm to 0 °C, and the mixture was stirred for 12 h. After oxidative quenching, GC–MS analysis of the crude reaction mix-

**SCHEME 1. Matteson Homologation Protocol of a Mixed Trialkylboranes**

ture revealed the presence of a plethora of products. In addition to products consistent with free-radical decomposition pathways such as iodo derivatives (iodocyclohexane and 1-iodohexane) and ligand dimerization products (dicyclohexane and 1-hexylcyclohexane) or simple ligand oxidation products (1-hexanol, cyclohexanol, and 2,3-dimethyl-2-butanol), we identified only a single migration product, namely 1-heptanol, coming from the migration of the primary *n*-hexyl group. No traces of cyclohexylmethanol or 2,2,3-trimethyl-1-butanol, deriving from the migration of the secondary or tertiary boron substituent, respectively, were observed. Of course, this result cannot be considered a conclusive evidence of a greater migratory aptitude of the primary alkyl group with respect to the secondary and tertiary ones. We recently reported more convincing results in a kind of vinylogous version of the same reaction. Mixed borane **3** was prepared as depicted in Scheme 2 and quaternized by tetrabutylammonium chloride to give the "ate" species **4** which exclusively underwent migration of the primary group to give a single allylic borane **5**.

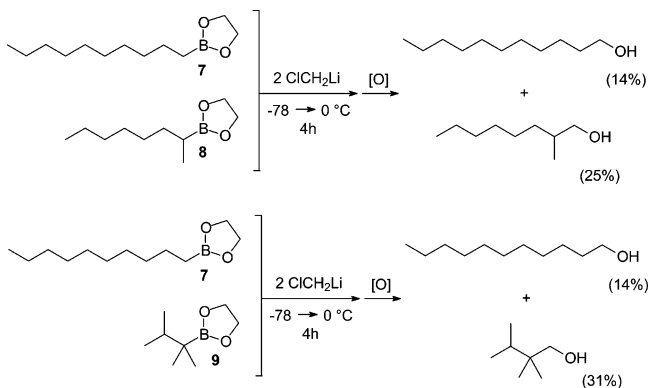
To check the presence of **5**, we carried out the quaternization reaction in the presence of benzaldehyde; the allylic intermediate **5** is immediately trapped by the

**SCHEME 2. Selective Primary Alkyl Group Migration from a Mixed "Ate" Species in a Vinylogous Matteson Homologation**

aldehyde, as confirmed by the isolation of the corresponding homoallylic alcohols **6**.<sup>24</sup>

These experiments confirm the trend generally observed in boron to carbon 1,2-shifts in "ate" species of type **A** (Table 1), where the migratory aptitude of primary alkyl groups is greater than that of tertiary groups.

**B. Experimental Studies on Boronates.** Considering that boronate homologation by quaternization with  $\text{ClCH}_2\text{Li}$  is a very well tested reaction,<sup>3</sup> we planned two experiments with the purpose of comparing the relative migratory aptitude of alkyl groups in "ate" species of type **B**, coming from cyclic boronates (Scheme 3).

**SCHEME 3. Competitive Matteson Homologation Experiments Using Primary, Secondary, and Tertiary Boronates**

For this purpose, we prepared 2-(1-decyl)-1,3,2-dioxaborolane (**7**), 2-(2-octyl)-1,3,2-dioxaborolane (**8**), and 2-(2,3-dimethyl-2-butyl)-1,3,2-dioxaborolane (**9**) as representative examples of boronates carrying a primary, a secondary, and a tertiary alkyl group on boron. Since only one alkyl group is transferred during the irreversible collapse of the "ate" species to the homologated boronate, we planned two intermolecular comparative experiments

(24) Lombardo, M.; Morganti, S.; Trombini, C. *Synlett* **2001**, 601. See also: Lombardo, M.; Morganti, S.; Trombini, C. *J. Org. Chem.* **2000**, 65, 8767.

(8) (a) Soderquist, J. A.; Najafi, M. R. *J. Org. Chem.* **1986**, 51, 1330. (b) Kabalka, G. W.; Slayden, S. W. *J. Organomet. Chem.* **1977**, 125, 274.

(9) Brown, H. C.; Kim, K.-W.; Cole, T. E.; Singaram, B. *J. Am. Chem. Soc.* **1986**, 108, 6761.

(10) (a) Brown, H. C.; Nambu, H.; Rogiæ, M. M. *J. Am. Chem. Soc.* **1969**, 91, 6852; (b) 6854; (c) 6855.

(11) Katz, J.-J.; Dubois, J.-E.; Lion, C. *Bull. Soc. Chim. Fr.* **1977**, 683.

(12) Slayden, S. W. *J. Org. Chem.* **1982**, 47, 2753.

(13) Slayden, S. W. *J. Org. Chem.* **1981**, 46, 2311.

(14) Brown, C. A.; Desai, M. C.; Jadhav, P. K. *J. Org. Chem.* **1986**, 51, 162.

(15) Brown, H. C.; Basavaiah, D.; Kulkarni, S. U.; Lee, H. D.; Negishi, E.-I.; Katz, J.-J. *J. Org. Chem.* **1986**, 51, 5270.

(16) Zweifel, G.; Fisher, R. P. *Synthesis* **1974**, 339.

(17) Pelter, A.; Hutchings, M. G.; Smith, K.; Williams, D. J. *J. Chem. Soc., Perkin Trans. 1* **1975**, 145.

(18) Zweifel, G.; Horng, A. *Synthesis* **1973**, 672. See also: Arase, A.; Hoshi, M. *J. Chem. Soc., Chem. Commun.* **1987**, 531.

(19) Midland, M. M.; Preston, S. B. *J. Org. Chem.* **1980**, 45, 747.

(20) Hoshi, M.; Arase, A. *J. Chem. Soc., Perkin Trans. 1*, **1993**, 2693.

(21) Brown, H. C. *Organic Syntheses via Boranes*; Wiley: New York, **1975**; pp 47–76.

(22) Brown, H. C.; Katz, J.-J.; Lane, C. F.; Negishi, E.-I. *J. Am. Chem. Soc.* **1975**, 97, 2799.

(23) Matteson, D. S.; Sing, R. P.; Schafman, B.; Yang, J.-J. *J. Org. Chem.* **1998**, 63, 4466. See also: Sadhu, K. M.; Matteson, D. S. *Organometallics* **1985**, 4, 1687.

under the same experimental conditions. In the first experiment, to an equimolar THF solution of **3** (0.27 M), **4** (0.27 M), and undecane (internal standard) was added  $\text{ICH}_2\text{Cl}$  (neat, 2 equiv) and then, at  $-78^\circ\text{C}$ ,  $n\text{-BuLi}$  (2 M in hexanes, 2 equiv).<sup>23</sup> After 10 min, the acetone–dry ice bath was replaced with an ice bath, and the reaction was stirred at  $0^\circ\text{C}$  for 4 h and eventually quenched with alkaline hydrogen peroxide. The crude extract in diethyl ether was analyzed by GC and by GC–MS, and the following yields were determined: undecanol (14%) and 2-methyl-1-octanol (25%). The second experiment was carried out in the same precisely reproduced conditions using **3** (0.27 M) and **5** (0.27 M). Final GC and GC–MS analysis revealed the presence of undecanol (14%) and 2,2,3-trimethyl-1-butanol (31%). The inspection of these results allowed us to conclude that the *hexyl* migrates 2.2 times as fast as the 1-decyl group and that 2-octyl migrates 1.8 times as fast as the 1-decyl group.

**C. Computational Details.** All the computations reported here have been carried out with the Gaussian 98 series of programs.<sup>25</sup> The structures of the various critical points have been fully optimized with the gradient method, and the nature of each critical point has been characterized by computing the harmonic vibrational frequencies. To choose a reliable computational approach, we first investigated the alkyl migration in the small model system **10** (Figure 2) either at the MP2 or DFT

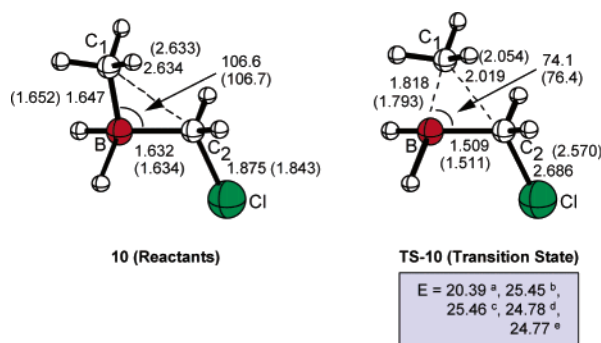


**FIGURE 2.** Structure of model system **10** and the corresponding transition state **TS-10**. The values of the most relevant geometrical parameters (angstroms and degrees) obtained at the B3PW91 and MP2 (in parentheses) levels and the energy ( $E$ , kcal·mol<sup>-1</sup>) of the transition state, relative to reactants, are reported (a, B3PW91 energy; b, MP2 energy; c, MP4 single-point at the MP2-optimized geometry; d, QCISD(T) single-point at the MP2-optimized geometry; MP2 single point at the B3PW91-optimized geometry).

level with the 6-31G\* basis set.<sup>25</sup> The B3PW91 hybrid functional, available in Gaussian 98, has been used. In the molecular system **10**, whose formal charge is  $-1$ , two

hydrogen atoms replace the alkyl groups bonded to boron and a methyl group emulates the migrating group.

The values of the most relevant geometrical parameters of **10** and of the transition state **TS-10** are collected in Figure 2. The energy of **TS-10**, relative to reactants (activation barrier) is also given. From these data it is evident that the values of the geometrical parameters computed with the B3PW91 functional are in good agreement with those obtained at the MP2 level. Also, the MP2 energy (25.45 kcal mol<sup>-1</sup>) agrees very well with the values obtained by means of MP4 or QCISD(T) single-point computations on the MP2-optimized structures (25.46 and 24.78 kcal mol<sup>-1</sup>, respectively). If we consider the MP4 and QCISD(T) energies as reference values, the DFT approach, as expected, underestimates the activation barrier (20.39 kcal mol<sup>-1</sup>). However, it is interesting to note that single-point MP2 computations on the B3PW91-optimized structures provide a barrier of 24.77 kcal mol<sup>-1</sup>. This result has prompted us to consider in the following discussion not only the DFT energies, but also the MP2 energies obtained from single-point computations on the B3PW91/6-31G\*-optimized structures.

**D. Computational Results: Chloromethyl Borate Systems.** We discuss the alkyl migration in the quaternary chloromethyl borate systems **11–13**. Here, the two hydrogen atoms bonded to boron of the small model system **10** are replaced by two methyl groups, while the primary, secondary, and tertiary migrating alkyl groups are emulated by a methyl (**11**), isopropyl (**12**), and *tert*-butyl (**13**) group, respectively. Moreover, we have examined two different situations: (a) a system corresponding to the simple chloromethyl borate anions **11a–13a** (gas-phase anion model-system) and (b) a system where the chloromethyl borate anions interact with the counterion  $\text{Li}^+$  **11b–13b** (gas-phase ion-pair model-system). A schematic representation of the structures of the various critical points with the values of the most relevant geometrical parameters is reported in Figure 3. The energy values, relative to reactants, are collected in Table 2. The effect of the solvent has been roughly evaluated by means of single-point computations with the polarized continuous model (PCM)<sup>26</sup> method on the optimum structures of the gas-phase ion-pair model-system. The emulated solvent is tetrahydrofuran (dielectric constant  $\epsilon = 7.58$ ), which is the solvent used in the experiments. The energy values including the solvent effects of the solvated species **11c–13c** are also reported in Table 2.

We discuss first in detail the most important structural features found for model system b (gas-phase ion-pair) and we compare them with those obtained for the simpler model system a (gas-phase anion). The following points are relevant:

(i) The presence of the counterion  $\text{Li}^+$  is not responsible for very large structural changes in the frame of both reactant and transition state. The most significant variations are observed for the three transition states **TS-11**, **TS-12**, and **TS-13** in the B–C<sub>1</sub>, B–C<sub>2</sub>, and C<sub>1</sub>–C<sub>2</sub> distances. For instance, after inclusion of the  $\text{Li}^+$  cation, the B–C<sub>1</sub> bond length decreases (from 1.838 Å in **TS-11a** to 1.728 Å in **TS-11b**), while the B–C<sub>2</sub> and C<sub>1</sub>–C<sub>2</sub>

(25) Gaussian 98, Revision A.6: Frisch, M. J.; Trucks, G. W.; Schlegel, H. B.; Scuseria, E. G.; Robb, M. A.; Cheeseman, J. R.; Zakrzewski, V. G.; Montgomery, J. A.; Stratmann, R. E.; Burant, J. C.; Dapprich, S.; Millam, J. M.; Daniels, A. D.; Kudin, K. N.; Strain, M. C.; Farkas, O.; Tomasi, J.; Barone, V.; Cossi, M.; Cammi, R.; Mennucci, B.; Pomelli, C.; Adamo, C.; Clifford, S.; Ochterski, J.; Petersson, G. A.; Cui, Q.; Morokuma, K.; Malick, D. K.; Rabuck, A. D.; Raghavachari, K.; Foresman, J. B.; Cioslowski, J.; Ortiz, J. V.; Stefanov, B. B.; Liu, G.; Liashenko, A.; Piskorz, P.; Komaromi, I.; Gomperts, R.; Martin, R. L.; Fox, D. J.; Keith, T.; Al-Laham, M. A.; Peng, C. Y.; Nanayakkara, A.; Gonzalez, C.; Challacombe, M.; Gill, P. M. W.; Johnson, B. G.; Chen, W.; Wong, M. W.; Andres, J. L.; Gonzalez, C.; Head-Gordon, M.; Replogle, E. S.; Pople, J. A. Gaussian, Inc., Pittsburgh, PA, 1998.

(26) Miertus, S.; Scrocco, E. Tomasi, J. *Chem. Phys.* **1981**, *65*, 239. Miertus, S.; Tomasi, J. *Chem. Phys.* **1982**, *65*, 239.



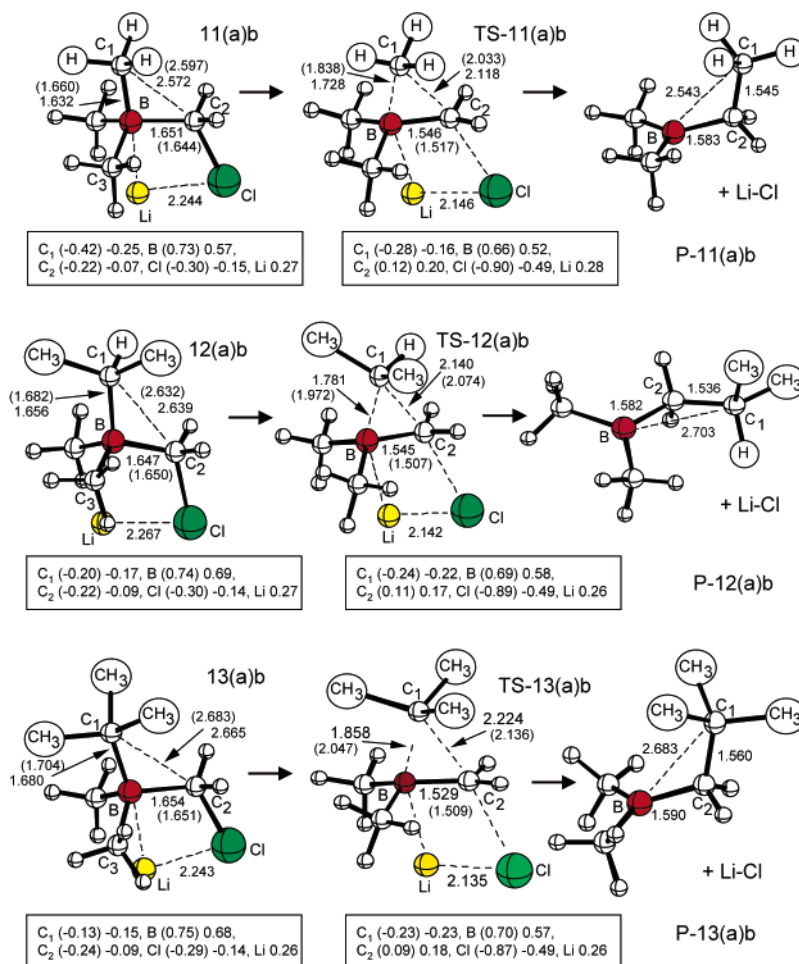


**FIGURE 3.** Structures of “ate” species **11**, **12**, and **13**, the corresponding transition states **TS-11**, **TS-12**, and **TS-13**, and products **P-11**, **P-12**, and **P-13**. The DFT values of the most relevant geometrical parameters (angstroms) and the net atomic charges obtained within model a (in parentheses) and model b are reported.

**TABLE 2.** Relative Energies (kcal mol<sup>-1</sup>) of Transition States and Products Computed for the Alkyl Migration in the System (H<sub>3</sub>C)<sub>2</sub>(R)CH<sub>2</sub>Cl (R = Me, *i*-Pr, *t*-Bu) at the B3PW91 and MP2 (Values in Parentheses) Computational Levels with the 6-31G\* Basis Set

	TS (transition state)	P (product)
anion model system		
<b>11a</b> (Me)	18.1 (24.8)	-8.6 (-3.3)
<b>12a</b> ( <i>i</i> -Pr)	22.5 (28.4)	-12.1 (-6.2)
<b>13a</b> ( <i>t</i> -Bu)	23.1 (29.6)	-11.0 (-5.7)
ion-pair model system		
<b>11b</b> (Me)	8.6 (12.9)	-16.5 (-11.9)
<b>12b</b> ( <i>i</i> -Pr)	8.9 (11.8)	-22.7 (-17.8)
<b>13b</b> ( <i>t</i> -Bu)	10.5 (13.7)	-23.6 (-18.8)
ion-pair model system with solvent effects <sup>a</sup>		
<b>11c</b> (Me)	7.1 (11.6)	-29.3 (-22.7)
<b>12c</b> ( <i>i</i> -Pr)	7.4 (10.5)	-35.3 (-27.1)
<b>13c</b> ( <i>t</i> -Bu)	9.0 (12.5)	-36.1 (-27.9)

<sup>a</sup> The emulated solvent is tetrahydrofuran ( $\epsilon = 7.58$ ).

distances increase (from 1.517 to 1.546 Å and from 2.033 to 2.118 Å, respectively, on going from **TS-11a** to **TS-11b**).

(ii) A planar C<sub>2</sub> carbon characterizes the three transition states and, in all cases, an inversion of configuration at C<sub>2</sub> and a retention of configuration at C<sub>1</sub> are observed. Furthermore, the transition states have always a reactant-like character. This is apparent by

comparing the lengths of the breaking (B-C<sub>1</sub>) and forming (C<sub>1</sub>-C<sub>2</sub>) bonds in reactants, transition states, and products. For instance, for the migration of a methyl group in the ion-pair system, the breaking B-C<sub>1</sub> bond is 1.632 Å in the reactant molecule **11b** and becomes 1.728 Å in the corresponding transition state **TS-11b**: this corresponds to only a 6% variation in the bond length. The new forming C<sub>1</sub>-C<sub>2</sub> bond is 2.118 Å in **TS-11b** and 1.545 Å in the product molecule **P-11b**, which corresponds to a much more significant change of about 37%. The same trend is observed for the isopropyl and *tert*-butyl groups.

(iii) Both the breaking and forming bonds become longer in the direction methyl → isopropyl → *tert*-butyl (the B-C<sub>1</sub> bond is 1.728, 1.781, and 1.858 Å in **TS-11b**, **TS-12b**, and **TS-13b**, respectively, while the corresponding values of the C<sub>1</sub>-C<sub>2</sub> bond are 2.118, 2.140, and 2.224 Å). The increasing steric demand of the migrating group, and the corresponding relief of steric compression around boron, is the most likely explanation for this trend.

(iv) The position of the counterion Li<sup>+</sup> corresponds to the minimum energy configuration, which makes possible a simultaneous interaction between lithium, the chlorine atom and the two carbon atoms of the nonmigrating methyl groups. It is interesting to point out that the lithium and chlorine atoms already strongly interact in

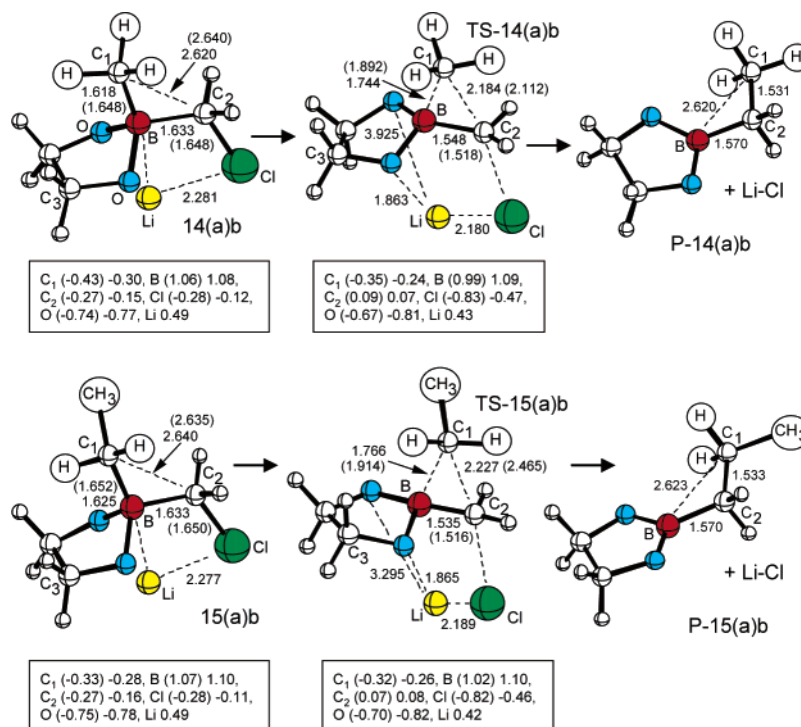


**FIGURE 4.** Structure of “ate” species **14** and **15**, the corresponding transition states **TS-14** and **TS-15**, and products **P-14** and **P-15**. The DFT values of the most relevant geometrical parameters (angstroms) and the net atomic charges obtained within model **a** (in parentheses) and model **b** are reported.

the reactants. The Li–Cl distance either in the reactant molecules (2.244 Å in **11b**, 2.267 Å in **12b**, 2.243 Å in **13b**) or in the transition state (2.146 Å in **TS-11b**, 2.142 Å in **TS-12b**, 2.135 Å in **TS-13b**) is only slightly longer than in the isolated Li–Cl molecule (2.060 Å).

(v) The analysis of the energy values (Table 2) shows that for model system **a** (anion) the activation barriers increase in the direction methyl → isopropyl → *tert*-butyl (18.1, 22.5 and 23.1 kcal mol<sup>−1</sup>, respectively). This would indicate a decreasing migratory aptitude on passing from the primary to the secondary and tertiary alkyl group. A similar trend has been found for the ion-pair system. In this case, the barrier is almost identical for methyl (**TS-11b**, 8.6 kcal mol<sup>−1</sup>) and isopropyl (**TS-12b**, 8.9 kcal mol<sup>−1</sup>) and then increases for the *tert*-butyl group (**TS-13b**, 10.5 kcal mol<sup>−1</sup>). No relevant variations are observed when we consider the solvent effect in the ion-pair model: 7.1 (**TS-11c**), 7.4 (**TS-12c**), and 9.0 kcal mol<sup>−1</sup> (**TS-13c**) are the corresponding activation energies. Thus, the more realistic model system, which accounts for the effects of the counterion and the solvent, provides the following information: primary and secondary alkyl groups migrate more easily than tertiary groups.

The MP2 activation barriers (Table 2 in parentheses) are, as expected, larger than the DFT values. However, they provide similar information. For model **a**, the barrier regularly increases along the direction primary → secondary → tertiary group. For the two models **b** and **c**, the barrier slightly decreases on passing from methyl to isopropyl, but decidedly increases for the *tert*-butyl group. Thus, again, the migratory aptitude is larger for primary and secondary groups than for tertiary groups.

These computational data agree both with the fact that, after quaternization of **1** and **3**, we only had evidence for the migration of the primary alkyl group, and with a number of reports in the literature (see Table 1). In particular, in entries 2, 4, 7, and 9 of Table 1 secondary alkyl groups are reported to act as migrating groups better than primary groups. In this case, a key factor could be the significantly higher exothermicity of the reaction observed for the migration of the isopropyl group. Also, it is interesting to point out that when we introduce the counterion in the model the absolute values of the activation energies significantly decrease and the exothermicity of the reaction increases. This would indicate a quite easy process, as found experimentally.

**E. Computational Modeling: Chloromethyl Boronate Systems.** The computational strategy used to investigate the chloromethyl boronate system **14–17** is similar to that illustrated in the previous section. Here a OCH<sub>2</sub>CH<sub>2</sub>O group replaces the two nonmigrating methyl groups bonded to boron. Methyl or ethyl, isopropyl, and *tert*-butyl groups are used as typical primary, secondary, and tertiary migrating alkyl groups. Again, we considered either a gas-phase anion model system (model **a**: simple “ate” species) or a gas-phase ion-pair model system (model **b**: “ate” species + Li<sup>+</sup>), and for model **b** we evaluated the effect of the solvent (PCM single-point computations). In Figures 4 and 5 we have schematically represented the structures of the various critical points and we have reported the values of the most important geometrical parameters. The energy values, relative to reactants, are collected in Table 3.

The analysis of these results shows that the chelating OCH<sub>2</sub>CH<sub>2</sub>O group bonded to boron does not cause dra-

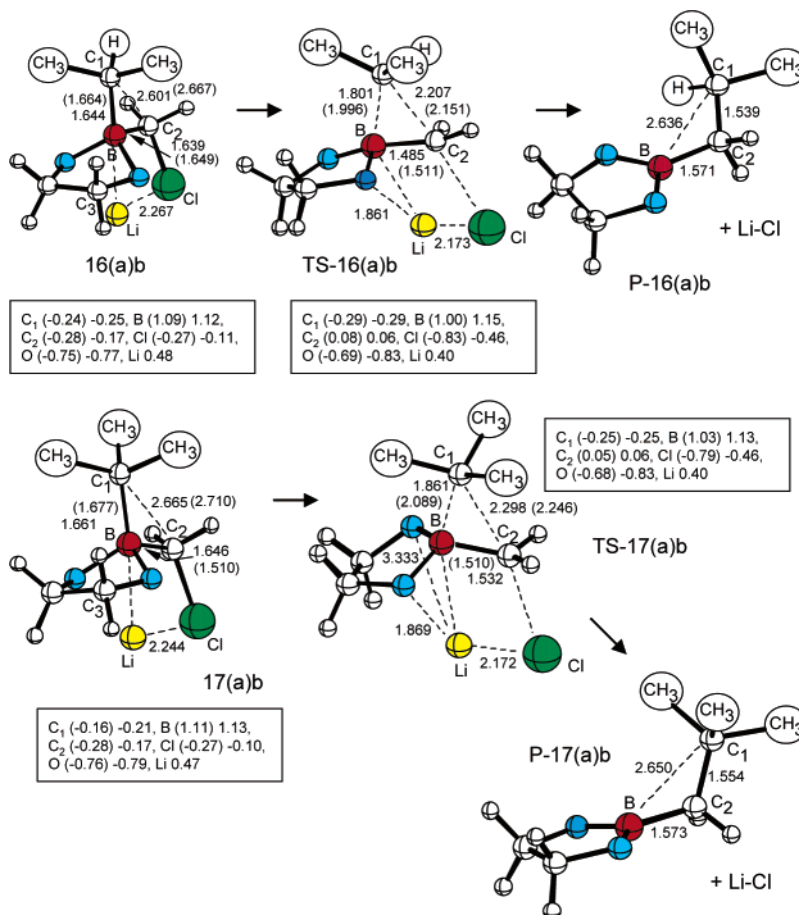


**FIGURE 5.** Structure of “ate” species **16** and **17**, the corresponding transition states **TS-16** and **TS-17**, and products **P-16** and **P-17**. The DFT values of the most relevant geometrical parameters (angstroms) and the net atomic charges obtained within model **a** (in parentheses) and model **b** are reported.

**TABLE 3.** Relative Energies (kcal mol<sup>-1</sup>) of Transition States and Products Computed for the Alkyl Migration in the System (OH<sub>2</sub>CCH<sub>2</sub>O)(R)CH<sub>2</sub>Cl (R = Me, Et, *i*-Pr, *t*-Bu) at the B3PW91 and MP2 (Values in Parentheses) Computational Levels with the 6-31G\* Basis Set

	TS (transition state)	P (product)
anion model system		
<b>14a</b> (Me)	20.8 (29.5)	-26.4 (-21.7)
<b>15a</b> (Et)	20.8 (29.9)	-27.1 (-21.9)
<b>16a</b> ( <i>i</i> -Pr)	22.3 (30.6)	-27.7 (-22.7)
<b>17a</b> ( <i>t</i> -Bu)	23.9 (32.8)	-26.9 (-22.1)
ion-pair model system		
<b>14b</b> (Me)	16.7 (24.6)	-21.2 (-14.0)
<b>15b</b> (Et)	16.4 (24.8)	-24.0 (-16.5)
<b>16b</b> ( <i>i</i> -Pr)	15.1 (22.0)	-28.6 (-21.0)
<b>17b</b> ( <i>t</i> -Bu)	13.3 (20.5)	-31.1 (-24.2)
ion-pair model system with solvent effects <sup>a</sup>		
<b>14c</b> (Me)	15.3 (24.0)	-32.9 (-24.6)
<b>15c</b> (Et)	15.0 (24.0)	-35.8 (-26.8)
<b>16c</b> ( <i>i</i> -Pr)	13.4 (20.9)	-40.3 (-30.7)
<b>17c</b> ( <i>t</i> -Bu)	11.6 (19.6)	-43.2 (-33.4)

<sup>a</sup> The emulated solvent is tetrahydrofuran ( $\epsilon = 7.58$ ).

matic changes in the molecular frame of reactants, transition states, and products with respect to the borate system. The transition states have an approximately C<sub>2</sub> planar structure and lead to an inversion of configuration at this atomic center. Also, they have again a strong reactant-like character as previously observed. For instance, for the ethyl migration, the breaking B–C<sub>1</sub> bond

shows a variation of about 8% on going from the reactant **15b** to the transition state **TS-15b** (this bond changes from 1.625 to 1.766 Å). The variation of the new forming C<sub>1</sub>–C<sub>2</sub> bond is much more significant, being 2.227 Å in **TS-15b** and 1.533 Å in the product **P-15b** (a variation of about 45%). Similar features are found for the other migrating groups. As pointed out in the previous section, the steric effect of the migrating group, which increases in the direction methyl → ethyl → isopropyl → *tert*-butyl, determines a lengthening of both the breaking B–C<sub>1</sub> and forming C<sub>1</sub>–C<sub>2</sub> bonds. In the ion-pair model **b**, for instance, the values of these bonds are as follows: 1.744 and 2.184 Å (methyl, **TS-14b**), 1.766 and 2.227 Å (ethyl, **TS-15b**), 1.801 and 2.207 Å (isopropyl, **TS-16b**), 1.861 and 2.298 Å (*tert*-butyl, **TS-17b**).

In the transition structures, the counterion coordinates to the substrate in a nonsymmetric way. A strong interaction is evident between lithium and only one of the two oxygen atoms. For instance, the two Li–O distances are 1.940 Å in the “ate” complex **14b** and become 1.863 and 3.295 Å in the transition state **TS-14b**. Similar values can be observed in **15b** and **TS-15b** (1.939 Å which becomes 1.865 and 3.295 Å), **16b** and **TS-16b** (1.945 Å and 1.861 and 3.177 Å, respectively), **17b** and **TS-17b** (1.948 Å and 1.869 and 3.333 Å, respectively). These nonsymmetric structures are real minima of the surface, as proved by the frequency computations (all real



frequencies), and the symmetric structure is a saddle-point between two equivalent minima. Furthermore, as observed for borates species of type **A**, the inclusion of the counterion in the model causes geometrical modifications that are more significant in the reactants than in the transition states. Here the presence of the cation always determines a shortening of the B–C<sub>1</sub> bonds and a lengthening of the B–C<sub>2</sub> bonds and, consequently, an increase of the reactant-like character.

More interesting is the effect of the counterion on the energies of both transition states and products. When the effects of the Li<sup>+</sup> cation are not included (model **a**), the migration activation energy is identical for the methyl and ethyl group (20.8 kcal mol<sup>−1</sup> for **TS-14a** and **TS-15a**) but increases for the isopropyl (22.3 kcal mol<sup>−1</sup> for **TS-16a**) and *tert*-butyl groups (23.9 kcal mol<sup>−1</sup> for **TS-17a**). Thus, the simpler model suggests a decreasing migratory aptitude along the direction primary → secondary → tertiary alkyl group, in contrast to the experimental evidence. When the effects of counterion are taken into account (ion-pair model **b**), this trend is reversed. In this case the activation energies become 16.7 and 16.4 kcal mol<sup>−1</sup> for **TS-14b** and **TS-15b**, respectively, 15.1 kcal mol<sup>−1</sup> for **TS-16b**, and 13.3 kcal mol<sup>−1</sup> for **TS-17b**. Also, the exothermicity of the reaction significantly increases on passing from the methyl to the *tert*-butyl group. The inclusion of the solvent effects does not change significantly these activation barriers and their trend (**14c–17c** in Table 3). Identical information is provided by the MP2 results. These data clearly indicates a migratory aptitude that increases from the primary to the tertiary group, in agreement with the experimental observations.

**F. Comparison between Relative Migratory Aptitudes in “Ate” Complexes A and B, Deriving from Boranes and Boronates.** The following important points arise from a comparison between the **A** species (**11–13**) and the **B** species (**14–17**):

(1) For a given migrating alkyl group, the activation barrier is larger for the boronate-derived **B** systems. The bond distances and the computed atomic charges (see Figures 3–5) show that the effect of the O–CH<sub>2</sub> groups bonded to boron is that of increasing the polarity of the B–C<sub>1</sub> bond and its strength with a consequent increase of the activation energy. This trend is observed within both model systems **a** and **b**.

(2) For both **A** (**11–13**) and **B** (**14–17**) species, the activation barrier decreases on passing from the isolated anion (model **a**) to the ion pair (model **b**). This effect is probably due to the stabilizing electrostatic interaction (existing only in model system **b**) between the Cl and Li atoms (**A** species) or between the Cl, Li, and O atoms (**B** species). It is evident from the computed charges that this contribution is larger in the transition state than in the reactants. The lengthening of the breaking C<sub>2</sub>–Cl bond caused by the counterion also concurs to lower the barrier.

(3) The analysis of the bond distances and of the computed atomic charges can help us to understand the inversion in the trend of the activation barriers on passing from model **a** to model **b** in boronate-derived compounds **14–17**. The length of the breaking B–C<sub>1</sub> bond in the reactant molecules **14–17** increases as the steric demand of the migrating group increases. This factor (a sort of “steric effect”) should favor the migration of the

most cumbersome alkyl group. A second factor (“charge effect”) originates from the negative charge that characterizes the migrating alkyl group in the reactants and transition states. This effect can be read following two different viewpoints: (i) The local negative charge on the migrating carbon atom decreases in the direction primary → secondary → tertiary as a result of charge dispersal on the branching groups by hyperconjugation. The higher the local charge on the migrating carbon, the higher is its nucleophilicity and, hence, its migratory aptitude. (ii) Alternatively, owing to the partial carbanionic nature of the migrating group, the migratory aptitude should follow the stability of these species and decrease in the direction primary > secondary > tertiary, i.e., the more stable the carbanion the easier the migration. It is evident that the two factors (steric hindrance and charge effect) play opposite roles and the final result depends on which factor does prevail.

A careful analysis of the local charge density on C<sub>1</sub> both in reagents **14a–17a** and transition states **TS-14a–TS-17a** shows that the methyl carbon always holds the highest charge, and that the negative charge on C<sub>1</sub> decreases in the direction primary → secondary → tertiary. More important, in model **b**, the lithium coordination significantly reduces the negative charge at the migrating carbon C<sub>1</sub>. Also, the variation of charge on C<sub>1</sub> decreases moving from methyl (**14b**) toward *tert*-butyl (**17b**). Thus, in model **a**, where the carbanionic nature of the alkyl group is more relevant, the migratory aptitude follows the trend of the carbanion stability. In the presence of the counterion (model **b**), where the carbanionic nature of the migrating group is less important and similar for the various migrating groups, the steric effect becomes dominant and the trend is reversed.

An analogous competition between steric and charge effects can be invoked to account for the partial variation of the migratory trends in the comparison between the isolated borates **11a–13a** and the corresponding ion pairs **11b–13b**.

## Conclusions

We have carried out a combined experimental and theoretical investigation at the MP2 and DFT levels of the boron-to-carbon 1,2-shift in quaternary borate and boronate species. To emulate the “ate” species involved in the migration process we have considered the two molecular systems **A** [Me<sub>2</sub>(R)BCH<sub>2</sub>Cl]<sup>−</sup> and **B** [OCH<sub>2</sub>CH<sub>2</sub>O-(R)BCH<sub>2</sub>Cl]<sup>−</sup> and we have investigated the migration of primary (R = Me, Et), secondary (R = *i*-Pr), and tertiary (R = *t*-Bu) alkyl groups. For both **A** and **B** species we have examined either the simple chloromethyl “ate” anions **11a–13a** or **14a–17a** (model **a**) or the chloromethyl anions interacting with the counterion Li<sup>+</sup> **11b–13b** and **14b–17b** (model **b**). For model **b**, the effect of the solvent has also been included using the polarized continuous model (PCM) method. Our results can be summarized as follows:

(a) The reaction proceeds via a concerted-type mechanism that explains the retention of configuration at the migrating group and the inversion at the migration terminus experimentally observed.

(b) The meaningful lowering of the activation barriers due to the presence of lithium, clearly accounts for the increased reaction rates observed in Matteson homolo-



gation reactions carried out in the presence of Lewis acids such as magnesium and zinc halides.

(c) The migration barrier increases on passing from borate to boronate-derived systems. This is due to an increase of the B–C<sub>1</sub> bond strength.

(d) When “ate” species **A** deriving from boranes are involved, theoretical data are consistent with both our experimental results and literature reports (Table 1) pointing out the following migratory aptitude: primary  $\approx$  secondary > tertiary.

(e) When “ate” species **B** deriving from boronates are considered, the experimental evidence obtained in the present work agrees with the results of model **b**, which includes the counterion effect (migratory aptitude trend: tertiary > secondary > primary).

According to our simple theoretical model, points d and e are the result of a delicate interplay between two opposite factors. The first factor (steric factor) favors the most sterically demanding migrating groups. A more pronounced lengthening of the B–C<sub>1</sub> bond marks its effect in structural terms. The second factor (charge factor) concerns the carbanionic nature of the migrating group. It favors the less substituted migrating carbons and its effect mainly resides in the local charge density found on C<sub>1</sub>.

## Experimental Section

**General Methods.** <sup>1</sup>H and <sup>13</sup>C NMR were recorded at 300 and 75 MHz, respectively, using tetramethylsilane as an internal standard. Chemical shifts are reported in ppm ( $\delta$ ) downfield from TMS. GC–MS analyses (70 eV) were performed with a quadrupole instrument. Solvents were dried using standard methods: THF was distilled from lithium aluminum hydride (LAH), CH<sub>2</sub>Cl<sub>2</sub> from P<sub>2</sub>O<sub>5</sub>, and pentane from sodium benzophenone immediately prior to use. All reactions were carried out in oven-dried glassware under an atmosphere of dry argon. All reagents were commercially available and were used without further purification, unless otherwise stated.

**2-Decyl[1,3,2]dioxaborolane (3).** A 1 M solution of dibromoborane in CH<sub>2</sub>Cl<sub>2</sub> (25 mL, 25 mmol) was slowly added to a stirred solution of 1-decene (5 mL, 25 mmol) in 12.5 mL of CH<sub>2</sub>Cl<sub>2</sub>. The resulting solution was refluxed for 3 h, allowed to reach rt, and transferred via cannula in a ice-cooled flask filled with water (4.5 mL) and ether (12.5 mL). The aqueous layer was extracted with pentane (3  $\times$  10 mL), and the combined organic layers were dried (Na<sub>2</sub>SO<sub>4</sub>) and concentrated at reduced pressure to afford a white solid that was purified by recrystallization from pentane to afford 2.47 g (13.3 mmol, 53%) of pure decyldihydroxyborane: mp 75–77 °C (lit.<sup>27</sup> mp 76–77 °C).

Ethylene glycol (0.34 mL, 6.65 mmol) was added to a solution of boronic acid (1.24 g, 6.65 mmol) in pentane (5 mL), and the reaction mixture was stirred at rt overnight. MgSO<sub>4</sub> was added, and the resulting suspension was stirred for 30 min, filtered, and evaporated to dryness to afford 1.36 g (6.42 mmol, 97%) of **3** as a clear oil that was used without further purifications: <sup>1</sup>H NMR (CDCl<sub>3</sub>)  $\delta$  0.8–0.95 (m, 3H), 1.20–1.35 (m, 16H), 1.35–1.50 (m, 2H), 4.2 (s, 4H); <sup>13</sup>C NMR (CDCl<sub>3</sub>)  $\delta$  9.2 (broad m), 12.6, 21.2, 22.5, 27.85, 27.95, 28.08, 28.16, 30.4, 30.9, 63.8. Anal. Calcd for C<sub>10</sub>H<sub>23</sub>BO<sub>2</sub>: C, 67.94; H, 11.88. Found: C, 67.91; H, 11.82.

**2-(1-Methylheptyl)[1,3,2]dioxaborolane (4).** Thionyl chloride (2.2 mL, 30 mmol) was slowly added at 0 °C to a solution of 2-octanol (4.8 mL, 30 mmol) in pyridine (2.7 mL, 33 mmol), and the reaction mixture was stirred overnight. Water was added (10 mL), and the aqueous layer was extracted with

CH<sub>2</sub>Cl<sub>2</sub> (3  $\times$  10 mL). The combined organic layers were dried (Na<sub>2</sub>SO<sub>4</sub>), filtered, and evaporated to dryness to afford a residue that was purified by distillation (bp 69–70 °C, 25 mmHg) to afford 2.1 g (14.2 mmol, 47%) of 2-chlorooctane: MS (70 eV) *m/z* 112 (18), 97 (10), 83 (71), 84 (47), 71 (17), 70 (100), 55 (79), 56 (56).

A small portion of pure 2-chlorooctane was added to a mixture of magnesium turnings (0.34 g, 14 mmol) in diethyl ether (3 mL). When the reaction had started, a solution of 2-chlorooctane (2.08 g, 14 mmol) in diethyl ether (17 mL) was slowly added at a rate that maintained a gentle reflux. After the addition was complete, the reaction mixture was stirred at 40 °C for 1 h and allowed to reach rt. The solution so obtained was transferred via cannula in a separatory funnel and slowly added at –78 °C to a solution of trimethoxyborane (4 mL, 35 mmol) in THF (30 mL). The reaction mixture was stirred at –78 °C for 1 h and quenched in an ice-cooled solution of aq NaHCO<sub>3</sub>. The aqueous layers were extracted with pentane, and the combined organic layers were dried (Na<sub>2</sub>SO<sub>4</sub>), filtered, and concentrated at reduced pressure to a small volume (~5 mL). To this solution of 2-(1-methylheptyl)-dihydroxyborane in pentane was added ethylene glycol (0.63 mL, 11 mmol), and the reaction mixture was stirred at rt overnight. MgSO<sub>4</sub> was added, and the resulting suspension was stirred for 30 min, filtered, and evaporated to dryness to afford 1.92 g (10.4 mmol, 74%) of **4** as a clear oil that was used without further purification: <sup>1</sup>H NMR (CDCl<sub>3</sub>)  $\delta$  0.80–1.00 (m, 3H), 1.00–1.10 (m, 3H), 1.20–1.35 (m, 10H), 1.35–1.50 (m, 1H), 4.2 (s, 4H); <sup>13</sup>C NMR (CDCl<sub>3</sub>)  $\delta$  14.1, 15.5, 22.7, 28.8, 29.4 (broad m), 29.6, 31.9, 33.3, 65.4. Anal. Calcd for C<sub>10</sub>H<sub>21</sub>BO<sub>2</sub>: C, 65.25; H, 11.50. Found: C, 65.33; H, 11.42.

**2-(1,1,2-Trimethylpropyl)[1,3,2]dioxaborolane (5).** A solution of 2,3-dimethyl-2-butene (2.4 mL, 20 mmol) in THF (8 mL) was slowly added at –15 °C to a solution of BH<sub>3</sub>·SMe<sub>2</sub> (2 mL, 20 mmol) in THF (8 mL). The reaction was stirred for 2 h at 0 °C and quenched with ice. The aqueous layer was extracted with diethyl ether, and the combined organic layers were dried (Na<sub>2</sub>SO<sub>4</sub>), filtered and concentrated at reduced pressure to a small volume. The residue was dissolved in pentane, ethylene glycol was added (0.92 mL, 16 mmol), and the reaction mixture was stirred at rt overnight. MgSO<sub>4</sub> was added, and the resulting suspension was stirred for 30 min, filtered, and evaporated to dryness to afford 2.31 g (15 mmol, 75%) of **5** as a clear oil that was used without further purification: <sup>1</sup>H NMR (CDCl<sub>3</sub>)  $\delta$  0.87 (d, *J* = 6.9 Hz, 6H), 0.91–0.96 (m, 6H), 1.14–1.20 (m, 1H), 4.2 (s, 4H). Anal. Calcd for C<sub>8</sub>H<sub>17</sub>BO<sub>2</sub>: C, 61.58; H, 10.98. Found: C, 65.64; H, 11.03.

**Intermolecular Comparative Experiments with Boronates 3–5.** An equimolar THF solution of **3** (0.27 M), **4** (0.27 M), and undecane (used as internal standard) was prepared, and a small aliquot was quenched with alkaline hydrogen peroxide and analyzed (GC/GC–MS) in order to characterize the reaction at the initial time *t*<sub>0</sub>. The solution was cooled at –78 °C, and ICH<sub>2</sub>Cl (neat, 2 equiv) was added followed by *n*-BuLi (2 M in hexanes, 2 equiv). After 10 min, the acetone–dry ice bath was replaced with an ice bath, and the reaction was stirred at 0 °C for 4 h and then quenched with alkaline hydrogen peroxide. The crude extract in diethyl ether was again analyzed by GC and by GC–MS to obtain peak areas at final time *t*<sub>1</sub>.

The same procedure was applied to the competitive analysis of **3** and **5**.

**Acknowledgment.** We thank the University of Bologna (funds for selected topics) and MURST (Rome, fondi ex-40%) for financial support.

**Supporting Information Available:** Geometrical parameters and detailed representation for the structures **11–17**, **TS11–17** and **P11–17**. This material is available free of charge via the Internet at <http://pubs.acs.org>.

(27) Thaisrivongs, S.; Wuest, J. D. *J. Org. Chem.* **1977**, *42*, 3.